A Lattice Boltzmann-Direct Forcing/Fictitious Domain Model for Brownian Particles in Fluctuating Fluids

Deming Nie[1,2] and Jianzhong Lin[1,2,*]

[1] *State Key Laboratory of Fluid Power Transmission and Control, Zhejiang University, Hangzhou 310027, China.*
[2] *College of Metrology and Technology Engineering, China Jiliang University, Hangzhou 310018, China.*

Abstract. The previously developed LB-DF/FD method derived from the lattice Boltzmann method and Direct Forcing/Fictitious Domain method is extended to deal with 3D particle's Brownian motion. In the model the thermal fluctuations are introduced as random forces and torques acting on the Brownian particle. The hydrodynamic interaction is introduced by directly resolving the fluid motions. A sphere fluctuating in a cubic box with the periodic boundary is considered to validate the present model. By examining the velocity autocorrelation function (VCF) and rotational velocity autocorrelation function (RVCF), it has been found that in addition to the two relaxation times, the mass density ratio should be taken into consideration to check the accuracy and effectiveness of the present model. Furthermore, the fluctuation-dissipation theorem and equipartition theorem have been investigated for a single spherical particle. Finally, a Brownian particle trapped in a harmonic potential has been simulated to further demonstrate the ability of the LB-DF/FD model.

1 Introduction

Particles suspended in fluids experience a random force due to the thermal fluctuations in the fluid around them in addition to the average hydrodynamic force. Brownian motion

*Corresponding author. *Email addresses:* `nieinhz@cjlu.edu.cn` (D. M. Nie), `linjz@cjlu.edu.cn`, `mecjzlin @zju.edu.cn` (J. Z. Lin)

may take place for those sub-micron/nanoscale particles. For many applications in microsystems for chemical and biological analysis, the ability to control and measure temperature inside microfluidic devices is critical since temperature often affects biological or chemical processes. Recent developments [1,2] demonstrate that the well-defined temperature dependence of the Brownian motion of nanoparticles could be used to present a temperature measurement technique which offers several benefits over existing methodologies. Brownian particle can be adopted to measure the local viscoelastic response of soft materials [3] or the topography of a surrounding polymer network [4]. The motion of a Brownian probe can also be used to characterize mechanical properties of molecular motors by analyzing the particle's trajectory [5]. Moreover, the biased Brownian motions or rectified Brownian motions, induced by an energy source [6] or by broken spatial reflection symmetry [7], provide a very effective technique for particle separation. Furthermore, it has been demonstrated [8,9] that nano-particles in a conventional base fluid, known as nanofluids, tremendously enhance the heat transfer characteristics of the original fluid. At the same time, many groups [10–12] have declared that Brownian motion is a key mechanism governing the thermal behavior of nanofluids. Besides, the theory of stochastic processes originated from Brownian motion have found wide applications in climate dynamics [13], stock market [14], traffic flow [15] and so on, which should go beyond Einstein's first consideration. Due to its importance in engineering applications, there has always been a great deal of interest in developing algorithms that can provide a better understanding of particle's Brownian motion. Especially in some cases [3–5], high resolution of Brownian motion is needed, which requires the numerical algorithms have the ability to observe the motion on short time scales ($t \ll \tau_D$, $\tau_D = a^2/D_0$, a is the spherical particle radius, D_0 is the particle diffusion coefficient).

Roughly speaking, the existing numerical methods for modeling particle's Brownian motion can be categorized by the treatment of particle's motion equations into three groups. (1) Langevin-type equation based method. Brownian dynamics (BD) [16] and Stokes dynamics (SD) [17,18] are the most important methods in this group. These methods treat the particle's motion by the Langevin equations without treatment of the fluid flow which indicates that random fluctuations are applied directly into the particles. For BD approximate expressions are used to model the hydrodynamic interactions and for SD the Rotne-Prager-Yamakawa tensors are used to express the hydrodynamic interactions. BD and SD are widely used numerical methods and achieved great success in the simulations of particles' Brownian motion. One of limitations of these methods may be that they cannot account for the short-time motion [19]. (2) DNS (Direct Numerical Simulation) method. In this group, the thermal fluctuations in the fluid, which result in the Brownian motion of particles, are modeled by adding a random stress tensor to Navier-Stokes equations. This method was called fluctuating hydrodynamics [20]. Solving the fluctuating hydrodynamic equations coupled with the particle equations of motion result in the Brownian motion of particles. In this method, the particles acquire random motion through the hydrodynamic force acting on its surface from the surrounding fluctuating fluid. Therefore, there is no need to add a random force term in the particles'

equations, unlike Langevin equations. Sharma and Patankar [21] have solved the fluctuating hydrodynamic equations through finite volume method and their numerical results include the Brownian displacements of a spherical particle and drag coefficient acting on the particle, which agree well with analytic values. Application of LBM coupled with fluctuating hydrodynamics to simulate particle's Brownian motion was first proposed by Ladd [22, 23], which is performed by adding a fluctuating term in the LB equation. These methods can successfully account for the short-time motion and deal with particles of irregular shape in a straightforward manner. In the late 1990's Ahlrichs and D*ü*nweg [24, 25] have applied the fluctuating lattice Boltzmann equations into the simulations of polymer solutions successfully. Other important references in this regard may be found in [26, 27]. Meanwhile, it should be stated here that in these methods, a random stress tensor required for a spatial grid, which needs a lot of random numbers for the fluctuating hydrodynamics, especially in 3D simulations. (3) Langevin-type equation based DNS method. In this group, Langevin equations are also adopted for the motion of the Brownian particles, while the hydrodynamic interaction is determined within a DNS framework. For instance, Yu et al. [28] extends the distributed Lagrange multiplier/fictitious domain (DLM/FD) method to deal with nanoparticles' Brownian motion to study the remarkable heat transfer in the nanofluids and his preliminary computational results support the argument that the micro-heat-convection induced by Brownian motion is primarily responsible for the unusually high heat conductivity of nanofluids. Also, Iwashita et al. [29] presented another numerical model to simulate the Brownian motion of solid particles, in which a Smoothed Profile (SP) method is used to solve fluid flow. In both studies [28, 29], Langevin equations are proposed for the Brownian particles. Iwashita et al. [29] have demonstrated that their model can account for the long-time behavior ($t > \tau_B$ for translational motion, $\tau_B = M/6\pi\mu a$, M is particle mass, a is particle radius, μ is fluid viscosity; $t > \tau_r$ for rotational motion, $\tau_r = J/8\pi\mu a^3$, J is moment of inertia) of particle's Brownian motion through numerical results of velocity autocorrelation function (VCF) and rotational velocity autocorrelation function (RVCF), which indicates that this method is effective only at $t > \tau_B$ or $t > \tau_r$. It should be pointed out here that in general the time scale τ_B or τ_r is much smaller than τ_D. In this respect, the Langevin-type equation based DNS method could be used to observe the motion on relative short time.

The lattice Boltzmann method (LBM) has been found applications in many areas of flow physics [30–32], especially in particle suspensions [33–40]. The bounce-back rule was first introduced to impose no-slip boundary conditions [22, 23], in which the particle surface is represented by the boundary nodes, which are essentially a set of the mid-points of the links between two fixed grids. It was proved robust and efficient for particulate flows, especially in the case of large number of particles. Later, the basic idea of the immersed boundary method (IBM) was incorporated successfully into LBM for the 2D and 3D fluid-particle systems, which has been known as IB-LBM [41, 42]. Recently, distributed Lagrange multipliers and fictitious domain (DLM/FD) method has been introduced into the framework of LB models for fluid-structure interactions [43, 44]. More recently, the LB-DF/FD method [45], which combines the ideas of the LBM and DF/FD

(Direct Forcing/Fictitious Domain) method, has been proposed for the 2D particle-fluid interaction problems. The aim of the present study is to extend the previous LB-DF/FD method from 2D to 3D cases, and provides an alternate approach for modeling particle's Brownian motion using the technique of Langevin-type equation based DNS scheme. To this end, we introduce thermal fluctuations by using white noise as random forces and torques for Brownian particles. Then, we would re-examine the long-time behavior of Brownian particle ($t > \tau_B$ or $t > \tau_r$) proposed by Iwashita et al. [29] and more deeply we want to provide some insight into the mechanism by which VCF or RVCF deviates from their theoretical results in the shorter time ($t < \tau_B$ or $t < \tau_r$). The present numerical model offers several benefits. First, in fluctuating hydrodynamics a random stress tensor is needed in Navier-Stokes equations, as a result it requires generating $\mathcal{O}(N^d)$ random numbers for numerical simulations with N^d spatial grids, while the present method requires only $\mathcal{O}(N_p)$ random numbers for a dispersion composed of N_p particles, which is much less than that of fluctuating hydrodynamics. Second, compared with Langevin-type equation based method, the present method can account for the hydrodynamic memory effects which play a key role in Brownian particles' short-time motion. It should be noted that the above two merits are true for all Langevin-type equation based DNS methods. Last, the present method makes use of LBM for solving fluid flow and consequently it preserves the merits of the LBM in simulating fluid flow [42].

The rest of the paper is organized as follows: Section 2 describes the LB-DF/FD model for particle's Brownian motion. In Section 3, firstly, the problem of decay of an initially posed translational velocity or rotational velocity of a sphere is utilized to verify the method; secondly, a sphere fluctuating in a cubic box with the periodic boundary is considered to examine the VCF and RVCF; finally, the motions of a Brownian particle in harmonic potentials is used to further check the validity of the method.

2 Numerical model

2.1 Lattice Boltzmann method

The fluid flow is solved by the LB method. The discrete LB equations of a single relaxation time model under external forces are described as

$$f_i(\mathbf{x}+\mathbf{e}_i\Delta t, t+\Delta t) - f_i(\mathbf{x},t) = -\frac{1}{\tau}\left[f_i(\mathbf{x},t) - f_i^{(0)}(\mathbf{x},t)\right] + \frac{\omega_i\Delta t}{c_s^2}(\boldsymbol{\lambda}\cdot\mathbf{e}_i), \qquad (2.1)$$

where $f_i(\mathbf{x},t)$ is the distribution function on the i-direction microscopic velocity $\mathbf{e}_i$, $f_i^{(0)}(\mathbf{x},t)$ is the equilibrium distribution function, $\boldsymbol{\lambda}$ is the external force, Δt is the time step of the simulation, τ is the relaxation time, c_s is the speed of sound and ω_i are weights related to lattice model. The fluid density ρ_f and velocity $\mathbf{u}$ are determined by the distribution function

$$\rho_f = \sum_i f_i, \qquad \rho_f\mathbf{u} = \sum_i f_i\mathbf{c}_i. \qquad (2.2)$$

For the D3Q15 lattice model used here, the discrete velocity vectors are

$$
\mathbf{e}_i = \begin{cases} (0,0), & i=0, \\ (\pm1,0,0)c,\ (0,\pm1,0)c,\ (0,0,\pm1)c, & i=1-6, \\ (\pm1,\pm1,+1)c,\ (\pm1,\pm1,-1)c, & i=7-14, \end{cases} \tag{2.3}
$$

where $c=\Delta x/\Delta t$, the speed of sound is defined as $c_s^2=c^2/3$, Δx is the lattice spacing. The equilibrium distribution function is chosen as

$$
f_i^{(0)}(\mathbf{x},t)=\omega_i\rho_f\left[1+\frac{3\mathbf{e}_i\cdot\mathbf{u}}{c^2}+\frac{9(\mathbf{e}_i\cdot\mathbf{u})^2}{2c^4}-\frac{3\mathbf{u}^2}{2c^2}\right], \tag{2.4}
$$

ω_i are chosen as the following values: $\omega_0=2/9$; $\omega_i=1/9$, $i=1\sim6$; $\omega_i=1/72$, $i=7\sim14$.

By performing a Chapman-Enskog expansion and in the low Mach number limit, the macroscopic mass and momentum equations can be recovered

$$
\nabla\cdot\mathbf{u}=0, \tag{2.5a}
$$

$$
\rho_f\left[\frac{\partial\mathbf{u}}{\partial t}+(\mathbf{u}\cdot\nabla)\mathbf{u}\right]=-\nabla p+\mu\nabla^2\mathbf{u}+\lambda. \tag{2.5b}
$$

The kinematic viscosity can be expressed as $\nu=(2\tau-1)(\Delta x)^2/6\Delta t$. For simplicity the lattice spacing Δx and time step Δt are both set be 1 in the present work.

2.2 LB-DF/FD method

Here we briefly explain the LB-DF/FD method in our numerical model since those are explained in detail elsewhere [45].

In DF/FD method, the interior domains of the particles are filled with the same fluids as the surroundings and a pseudo body force λ is introduced to enforce the interior (fictitious) fluids to satisfy the constraint of rigid body motion, as described by

$$
\mathbf{u}=\mathbf{U}+\omega_s\times\mathbf{r} \qquad \text{(the particle inner domain, P)}, \tag{2.6}
$$

where $\mathbf{U}$ and ω_s are the particle translational velocity and angular velocity, respectively. Moreover, in DF/FD method, a certain number of Lagrangian nodes are distributed to represent the particle in the simulations, while an Eulerian mesh is used for the fluid.

The Brownian motion of a particle with mass M and moment of inertia $\mathbf{J}$ is governed by Newton's equations

$$
M\frac{d\mathbf{U}}{dt}=\mathbf{F}^H+\mathbf{F}^B+\mathbf{F}^E, \tag{2.7a}
$$

$$
\frac{d(\mathbf{J}\cdot\omega_s)}{dt}=\mathbf{T}^H+\mathbf{T}^B, \tag{2.7b}
$$

where $\mathbf{F}^H$ and $\mathbf{T}^H$ are the hydrodynamic forces and torques on the particle, respectively, defined as

$$\mathbf{F}^H = \int_{\partial P} \mathbf{n} \cdot \sigma \, ds, \qquad \mathbf{T}^H = \int_{\partial P} \mathbf{r} \times (\mathbf{n} \cdot \sigma) \, ds, \tag{2.8}$$

where σ is the fluid stress tensor, $\mathbf{n}$ is the unit outward normal on the particle surface and $\mathbf{r}$ is the position vector with respect to the particle mass center. $\mathbf{F}^B$ and $\mathbf{T}^B$ are the random forces and torques due to thermal fluctuations which are defined in the following section. $\mathbf{F}^E$ denotes other external forces.

Based on a direct-forcing scheme, the forcing term exerted on the Lagrangian points in the particle domain can be expressed as

$$\lambda^{n+1} = \rho_f \frac{\mathbf{u}^{n+1} - \mathbf{u}^*}{\Delta t} = \rho_f \frac{\mathbf{U}^{n+1} + \omega_s^{n+1} \times \mathbf{r} - \mathbf{u}^*}{\Delta t}, \tag{2.9}$$

where $\mathbf{u}^*$ is a temporary velocity which satisfies the momentum equation (2.5b) with zero body-force.

From (2.5b)-(2.8), one can obtain the equations for updating particle's Brownian motion

$$M \frac{\mathbf{U}^{n+1}}{\Delta t} = (M - M') \frac{\mathbf{U}^n}{\Delta t} + \int_P \rho_f \frac{\mathbf{u}^*}{\Delta t} d\Omega + \mathbf{F}^{B^{n+1}} + \mathbf{F}^{E^{n+1}}, \tag{2.10a}$$

$$\frac{\mathbf{J} \cdot \omega_s^{n+1}}{\Delta t} = \frac{(\mathbf{J} - \mathbf{J}') \cdot \omega_s^n}{\Delta t} - \omega_s^n \times [(\mathbf{J} - \mathbf{J}') \cdot \omega_s^n] + \int_P \rho_f \mathbf{r} \times \frac{\mathbf{u}^*}{\Delta t} d\Omega + \mathbf{T}^{B^{n+1}}, \tag{2.10b}$$

where M' and $\mathbf{J}'$ are expressed as

$$M' = \int_P \rho_f d\Omega, \qquad \mathbf{J}' = \int_P \rho_f \mathbf{r} \times \mathbf{r} d\Omega. \tag{2.11}$$

As shown from (2.10a) and (2.10b), the hydrodynamic forces and torques exerted on the particle does not appear explicitly and as a result it's unnecessary to calculate them to update the particle's motion.

The whole problem is decoupled into the fluid and solid particle sub-problems with the fractional step scheme, which includes the following steps:

1. Calculate $f^*(\mathbf{x}, t)$ from Eq. (2.1) without the body force λ and then $\mathbf{u}^*$ from Eq. (2.2).

2. Based on Eqs. (2.10a) and (2.10b), calculate translational velocity $\mathbf{U}$ and angular velocity ω_s.

3. Update pseudo body-force λ^{n+1} inside the particle domain through Eq. (2.9).

4. Introduce body-force λ^{n+1} into Eq. (2.1) and calculate $f(\mathbf{x}, t)$ without collision, then the new ρ_f and $\mathbf{u}$ determined.

2.3 Brownian forces and torques

In the present model Brownian forces $\mathbf{F}^B$ and torques $\mathbf{T}^B$, due to thermal fluctuations, are introduced as white noise, in the same way as the Langevin equation (LE) does. They have the following properties:

$$< F_i^B(t) >= 0, \quad < F_i^B(t)F_j^B(t') >= C_1\delta_{ij}\delta(t-t'), \quad i,j = x,y,z, \tag{2.12a}$$

$$< T_i^B(t) >= 0, \quad < T_i^B(t)T_j^B(t') >= C_2\delta_{ij}\delta(t-t'), \quad i,j = x,y,z, \tag{2.12b}$$

where the angle brackets denote taking an average over an equilibrium ensemble, C_1 and C_2 are parameters to control the temperature. Eq. (2.12) indicates that Brownian forces $\mathbf{F}^B$ and torques $\mathbf{T}^B$ are Markovian, which indicates that we neglected their memory effects. In the simulations, F_i and T_i are generated by a Gaussian random number generator with the desired mean and variance.

The translational temperature $K_B T^V$ and rotational temperature $K_B T^\Omega$ are determined in the same way as [29]. First, the translational diffusion coefficient D^V and rotational diffusion coefficient D^Ω are calculated in the numerical simulations through the following Green-Kubo integrals:

$$D^V = \frac{1}{3}\int_0^\infty < \mathbf{U}(0)\cdot\mathbf{U}(t) > dt, \qquad D^\Omega = \frac{1}{3}\int_0^\infty < \mathbf{\Omega}(0)\cdot\mathbf{\Omega}(t) > dt. \tag{2.13}$$

Then the Stokes-Einstein diffusion coefficients of a spherical particle with radius a, $D^V = K_B T^V/6\pi\mu a$ for the translational motion and $D^\Omega = K_B T^\Omega/8\pi\mu a^3$ for the rotational motion, can be used to define the temperatures $K_B T^V$ and $K_B T^\Omega$. The parameters C_1 and C_2 in Eq. (2.8) are chosen to make sure $K_B T^V = K_B T^\Omega$.

Widom [46] studied the behavior of a spherical Brownian particle in a viscous fluid by using the generalized Langevin equation (GLE), which has also been studied by Hauge et al. [47] and Hinch [48]. It has been found that the Brownian forces or torques autocorrelation function are not proportional to the Dirac δ function, unlike Eq. (2.12), which indicates that Brownian forces $\mathbf{F}^B$ and torques $\mathbf{T}^B$ are non-Markovian. As a fact, the Markovian effects due to Eq. (2.12) might cause deviations from theoretical results. Iwashita et al. [29] have numerically investigated these deviations by SPM coupling with Langevin equations and proposed a long-time behavior. We aim to re-examine this long-time behavior and take further investigations.

3 Results and discussion

For the spherical particle, the Lagrangian nodes are distributed on the concentric spherical surfaces. On each surface, the distribution of the nodes is determined using the method suggested by Yu [49] and Uhlmann [50]. For a given value of N_l, run a simulation of the motion of point-particles confined to the surface of a sphere. These points are moving under a mutual repulsive force which is proportional to the inverse of the

square of the inter-particle distance. After several runs an equilibrium configuration can be obtained. In the present method, the number of the Lagrangian points on ith surface is set to be $N_b i^2$, here N_b being the number of nodes on the first surface. Let N_s denote the number of the surfaces, the total number of the Lagrangian nodes for a sphere is $N_l = 1 + N_b N_s (N_s + 1)(2N_s + 1)/6$.
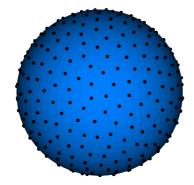

Figure 1: Arrangements of Lagrangian points for a spherical particle (only the points on one layer is shown).

It should be remarked that the arrangement of Lagrangian nodes as shown in Fig. 1 is one of the possible ways to distribute Lagrangian points. Moreover, the numbers of Lagrangian nodes or the numbers of the surfaces used in the present work are not the unique answer. There's no a general theory or rule to determine them. Numerical simulations have suggested that the numbers of Lagrangian nodes can be chosen just to make $\Delta V_l (\Delta V_l = V_p / N_l \cdot x_3$, V_p is the particle volume) not too large or too small, for the sake of numerical stability.

As an initial test of the present model, Brownian motion of a single sphere in a periodic box has been numerically investigated. In Fig. 2, the decay of an initially posed translational velocity $U(0)$ or rotational velocity $\Omega(0)$ of the sphere is compared with the analytical solutions for different periodic unit cells from 18^3 to 72^3. The analytical solutions are based on an inverse Laplace transform of the frequency-dependent equations of motion [47]. Both of them are normalized by their $t = 0$ values. The initial values of $U(0)$ and $\Omega(0)$ for decay are both set to be 0.01 (in lattice unit). Other parameters are summarized as follows: $a = 2.65$, $\nu = 1/6$, $\rho_f = 1$, $\rho_p = 11$, $N_s = 2$, which are similar to those of Ladd [23]. The results show that the length of simulated periodic box has significant effect on the decay of translational velocity but little effect on the decay of rotational velocity. Furthermore, from Fig. 2 good agreement between numerical and theoretical results can be observed over the whole time domain for periodic box of 72^3, which has been chosen through the whole numerical simulations to make sure that the results are unaffected by the periodic boundary conditions.

Besides, in order to demonstrate the effect of arrangements of Lagrangian nodes, three kinds of arrangements referring to $N_b = 8,10$ and 12 have been taken into account. Numerical results have been shown in Fig. 3 for translational velocity and rotational velocity,

respectively. The results indicate that the influences of the arrangements of Lagrangian points are negligible.

Fig. 4 shows the velocity autocorrelation function (VCF) $<U(0)U(t)>$ and rotational velocity autocorrelation function (RVCF) $<\Omega(0)\Omega(t)>$ of the same sphere. The temperature has been set to be $K_BT \approx 1.1 \times 10^{-3}$. As is known, Langevin equation (LE) leads to an exponential decay both in VCF and RVCF because it completely neglects the hydrodynamic memory effects. In Fig. 4 it can be seen that our numerical results agree well with the analytical solution based on an inverse Laplace transform of the frequency-dependent equations of motion [47] rather than the exponential LE results, which indicates that the hydrodynamic memory effects are accurately taken into account in the present model. It should be stated that in [29] two relaxation time parameters have been used to describe their numerical results, $\tau_B = M/6\pi\mu a$ for translational Brownian motion and $\tau_r = J/8\pi\mu a^3$ for rotational Brownian motion, respectively. They have shown that the deviations become notable for $t < \tau_B$ or $t < \tau_r$, while the agreements between the numerical results and the analytical solutions are excellent for $t > \tau_B$ or $t > \tau_r$. However, in our results the deviations are not very obvious, even when t is small. Good agreement can be observed almost over the whole time domain as shown in Fig. 4.

To assist clarify this problem, we have also conducted another simulation with the same computational parameters as the above except $\rho_p = 1$ and $K_BT \approx 1.0 \times 10^{-3}$. The results have been shown in Fig. 5, which is consistent with [29]. Almost the same conclusion can be drawn from Fig. 5. However, by comparing numerical results with analytical solutions in detail, it can be found that the deviations at $t < \tau_B$ or $t < \tau_r$ are more notable for $\rho_p = 1$ than for $\rho_p = 11$. Let's introduce another relaxation time $\tau_v = a^2/v$, which is usually used to characterize the fluid inertia. By comparing τ_B which characterizes the particle inertia with τ_v, one can get $\tau_B/\tau_v = 2\rho_p/9\rho_f$. Therefore, as ρ_p/ρ_f increases the particle inertia influences the Brownian motion more than the fluid inertia, as a result, the Markovian effects become more important, which leads to the fact that Brownian forces $\mathbf{F}^B$ and torques $\mathbf{T}^B$ defined by Eq. (2.11) can account for the Brownian motion more accurately for $\rho_p/\rho_f = 11$ than for $\rho_p/\rho_f = 1$. Moreover, it should be mentioned that as ρ_p/ρ_f approaches infinity, non-Markovian effects can be completely neglected and LE dominates the Brownian motion, and of course the deviations would disappear no matter how much τ_B is. The same conclusion can be made for rotational Brownian motion if one get $\tau_r/\tau_v = \rho_p/15\rho_f$.

A basic relation between the relaxation response of a dragged particle and the VCF of a Brownian particle is the fluctuationCdissipation theorem. It should be noted that the analytical solutions in Fig. 3 are identical to those in Fig. 4, in other words, within the statistical error the velocity correlation functions are identical to the steady decay of the translational and rotational velocities of the same sphere. Therefore, by taking the mass density ratio ρ_p/ρ_f into account our simulations satisfy the fluctuation-dissipation theorem at least for $t > \tau_B$ or $t > \tau_r$.

It has been shown that thermal equilibrium between the Brownian particle and the surrounding fluid molecular will reach and that an equi-partition of energy for each de-
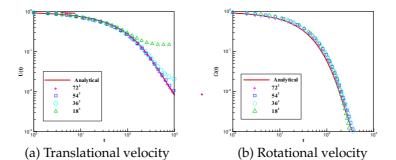
(a) Translational velocity

(b) Rotational velocity

Figure 2: Decay of an initially posed translational velocity or rotational velocity of a sphere of $a = 2.65$ and $\rho_p = 11$ for different periodic boxes.

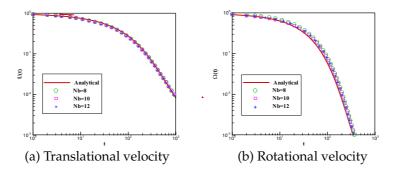(a) Translational velocity

(b) Rotational velocity

Figure 3: Decay of an initially posed translational velocity or rotational velocity of a sphere of $a = 2.65$ and $\rho_p = 11$ for different N_b number.
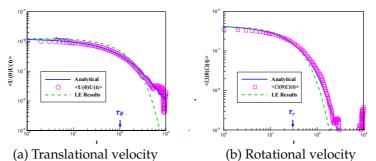

(a) Translational velocity

(b) Rotational velocity

Figure 4: Velocity autocorrelation function $<U(0)U(t)>$ and $<\Omega(0)\Omega(t)>$ of a sphere of $a = 2.65$ and $\rho_p = 11$.

(a) Translational velocity

(b) Rotational velocity
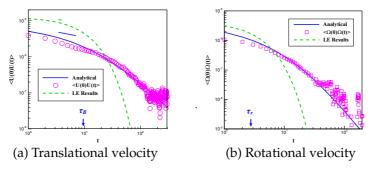
Figure 5: Velocity autocorrelation function $<U(0)U(t)>$ and $<\Omega(0)\Omega(t)>$ of a sphere of $a = 2.65$ and $\rho_p = 1$.

gree of freedom for both translational and rotational Brownian motion will be observed, which can be described as [47]

$$<U^2(0)>=<V^2(0)>=<W^2(0)>\frac{K_BT}{M_e}, \tag{3.1a}$$

$$<\Omega^2(0)>=<\Theta^2(0)>=<Y^2(0)>=\frac{K_BT}{J}, \tag{3.1b}$$

where U, V and W refer to translational velocity of x, y and z coordinate, Ω, Θ and Y refer to rotational velocity of x, y and z coordinate, respectively. M_e is the effective mass, described as $M_e = M + 2\pi a^3 \rho_f / 3$. It should be pointed out that Eq. (3.1a) is in contradiction with the equipartition theorem because the particle mass M instead of the effective mass Me would be expected in Eq. (3.1a). An equi-partition of energy for both translational and rotational motion at x, y and z coordinate can be observed in both cases after a certain run time, as displayed in Fig. 6. Moreover, it can be seen that the equi-partition of energy at x, y and z coordinate is reached earlier for rotational motion than for translational motion. Not surprisingly, it takes more time to reach thermal equilibrium of all three degrees of freedom in both translational and rotational motion for $\rho_p = 11$ than for $\rho_p = 1$ due to particle inertia. However, thermal equilibrium between solid particle and fluid has not been found since the mean-square velocities (MSV) of translational motion or rotational motion deviate from K_BT/M_e or K_BT/J quantitatively, which is clearly shown in Fig. 6. In additions, the MSV of translational motion are about 16% less than K_BT/M_e for $\rho_p = 1$ and about 11% less than K_BT/M_e for $\rho_p = 11$. The results are consistent with the conclusion that as ρ_p/ρ_f increases the present model can account for particle's Brownian motion more accurately. The similar observations about thermal equilibrium between solid particle and fluid have also been obtained by Ladd [23] through the fluctuating lattice-Boltzmann equations. In his simulations, the temperatures characterizing translation and rotation are similar, but typically 10-20% less than the effective temperature of the fluid fluctuations.

In order to further demonstrate the ability of the present LB-DF/FD model, a Brownian particle trapped in a harmonic potential has been considered. This problem is usually adopted to describe a Brownian particle confined to a restricted volume. The harmonic potential is introduced by adding a harmonic force

$$\mathbf{F}^{HP} = -k(\mathbf{R} - \mathbf{R}^{eq}), \tag{3.2}$$

where $\mathbf{R}^{eq}$ is its equilibrium position and k the spring constant.

One of the most important results in this problem is the mean-square displacement (MSD) of Brownian particle which has been given by [51]

$$\lim_{t\to\infty}<\Delta r^2(t)>\frac{2k_BT}{k}, \tag{3.3}$$

where $<\Delta r^2(t)>=\langle|\mathbf{R}(t)-\mathbf{R}(0)|^2\rangle/3$. In the simulations the parameters are summarized as follow: $a=2.65$, $\nu=1/6$, $\rho_p=11$, $K_BT\approx 1.0\times10^{-3}$. Eight spring constants k range from
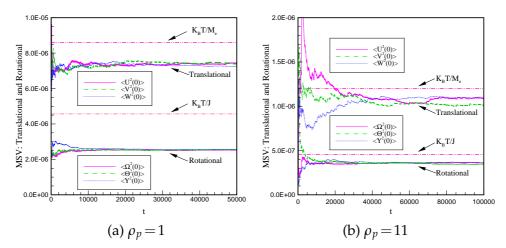
Figure 6: Time evolutions of the mean-square velocities (MSV) for $\rho_p = 1$ and 11.
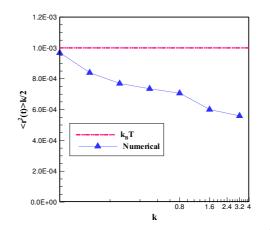

Figure 7: The spring constant dependence of the $\lim_{t \to \infty} < \Delta r^2(t) > k/2$.

0.05 to 3.2 have been taken into account, and the corresponding temperature KBT derived from $\lim_{t \to \infty} < \Delta r^2(t) > k/2$ are plotted in Fig. 7. Obviously, the result approaches $K_B T$ as $k \to 0$ and is consistent with the results obtained from the diffusion coefficient for a Brownian particle.

4 Conclusions

In this paper, the lattice Boltzmann-Direct Forcing/Fictitious Domain method is extended to solve the 3D particle Brownian motion. Langevin equations are considered for the motion of the Brownian particle, while the hydrodynamic forces and torques are determined in a DNS framework. By examining the velocity autocorrelation function (VCF) and rotational velocity autocorrelation function (RVCF), it has been found that the numerical

results agree well with analytical solutions at long-time ($t > \tau_B$ or $t > \tau_r$), which is consistent with the previous numerical results. At the same time, the mass density ratio ρ_p/ρ_f plays a key role in the present simulations. As ρ_p/ρ_f increases, the particle inertia influences the Brownian motion more than the fluid inertia, which makes the Langevin equations become more accurate. Therefore, if ρ_p/ρ_f is large enough the numerical results may agree well with analytical solutions even $t < \tau_B$ or $t < \tau_r$. The mean-square velocities (MSV) of translational motion or rotational motion also confirmed this conclusion.

On the other hand, it should be noted that this study has been only for a single spherical particle case. Extending the present LB-DF/FD model to non-spherical particle and many particles system should be the future work. Moreover, the mechanism of thermal equilibrium between the particle and fluid is not fully developed, and should be examined more deeply in the future work.

Acknowledgments

References

[1] J. S. Park, C. K. Choi and K. D. Kihm, Temperature measurement for a nanoparticle suspension by detecting the Brownian motion using optical serial sectioning microscopy (OSSM), Meas. Sci. Technol., 16 (2005), 1418–1429.

[2] K. Chung, J. K. Cho, E. S. Park, V. Breedveld and H. Lu, Three-dimensional in situ temperature measurement in microsystems using Brownian motion of nanoparticles, Anal. Chem., 81 (2009), 991–999.

[3] F. C. MacKintosh and C. F. Schmidt, Microrheology, Curr. Opin. Coll. Interface. Sci., 4(1999), 300–307.

[4] C. Tischer, S. Altmann, S. Fisinger, J. K. H. Hör̈ber, E. H. K. Stelzer and E.-L. Florin, Three-dimensional thermal noise imaging, Appl. Phys. Lett., 79 (2001), 3878–3880.

[5] S. Jeney, E. H. K. Stelzer, H. Grüı̈bmuller and E.-L. Florin, Mechanical properties of single motor molecules studies by three-dimensional thermal force probing in optical tweezers, Chem. Phys. Chem., 5 (2004), 1150–1158.

[6] R. Dean Astumian, Thermodynamics and kinetics of a Brownian motor, Science, 276 (1997), 917–922.

[7] I. Dere'nyi and R. D. Astumian, AC separation of particles by biased Brownian motion in a two-dimensional sieve, Phys. Rev. E., 58 (1998), 7781–7784.

[8] P. Keblinski, S. R. Phillpot, S. U. S. Choi and J. A. Eastman, Mechanisms of heat flow in suspensions of nano-sized particles (nanofluids), Int. J. Heat. Mass. Trans., 45 (2002), 855–863.

[9] S. Lee, S. U. S. Choi, S. Li and J. A. Eastman, Measuring thermal conductivity of fluids containing oxide nanopartieles, J. Heat. Trans., 121 (1999), 280–289.

[10] R. Prasher, P. Bhattacharya and P. E. Phelan, Thermal conductivity of nanoscale colloidal solutions (nanofluids), Phys. Rev. Lett., 94 (2005), 025901.

[11] S. P. Jang and S. U. S. Choi, Role of Brownian motion in the enhanced thermal conductivity of nanofluids, Appl. Phys. Lett., 84 (2004), 4316–4318.

[12] P. Bhattacharya, S. K. Saha, A. Yadav and P. E. Phelan, Brownian dynamics simulation to determine the effective thermal conductivity of nanofluids, J. Appl. Phys., 95 (2004), 6492–6494.

[13] D. M. Sonechkin, Climate dynamics as a nonlinear Brownian motion, Int. J. Bifurcation. Chaos. Appl. Sci. Eng., 8 (1998), 799–803.

[14] T. Sottinen, Fractional Brownian motion, random walks and binary market models, Finance. Stochast., 5 (2001), 343–355.

[15] Y. Shiftan, K. Button and P. Nijkamp, Transportation Planning, Ediward Elgar Publishing, Inc., U.K., 2007.

[16] D. L. Ermak and J. A. McCammon, Brownian dynamics with hydrodynamic interactions, J. Chem. Phys., 69 (1978), 1352–1360.

[17] J. F. Brady and G. Bossis, Self-diffusion of Brownian particles in concentrated suspensions under shear, J. Chem. Phys., 87 (1987), 5437–5448.

[18] J. F. Brady, G. Bossis, Stokesian dynamics, Annu. Rev. Fluid. Mech., 20 (1988), 111–157.

[19] A. J. C. Ladd, Short-time motion of colloidal particles: numerical simulation via a fluctuating Lattice-Boltzmann equation, Phys. Rev. Lett., 70 (1993), 1339–1342.

[20] L. D. Landau and E. M. Lifshitz, Fluid Mechanics, London, Pergamon Press, 1959.

[21] N. Sharma and N. A. Patankar, Direct numerical simulation of the Brownian motion of particles by using fluctuating hydrodynamic equations, J. Comput. Phys., 201 (2004), 466–486.

[22] A. J. C. Ladd, Numerical simulations of particulate suspensions via a discretized Boltzmann equation part I: theoretical foundation, J. Fluid. Mech., 271 (1994), 285–310.

[23] A. J. C. Ladd, Numerical simulations of particulate suspensions via a discretized Boltzmann equation part II: numerical results, J. Fluid. Mech., 271 (1994), 311–339.

[24] P. Ahlrichs and B. Dü nweg, Lattice-Boltzmann simulation of polymer-solvent systems, Int. J. Mod. Phys. C., 9 (1998), 1429–1438.

[25] P. Ahlrichs and B. Dünweg, Simulation of a single polymer chain in solution by combining lattice Boltzmann and molecular dynamics, J. Chem. Phys., 111 (1999), 8225–8239.

[26] B. Dünweg, U. D. Schiller and A. J. C. Ladd, Statistical mechanics of the fluctuating lattice Boltzmann equation, Phys. Rev. E., 76 (2007), 036704.

[27] B. Dünweg and A. J. C. Ladd, Lattice Boltzmann simulations of soft matter systems, Adv. Poly. Sci., 221 (2009), 89–166.

[28] Z. S. Yu, X. M. Shao and A. Wachs, A fictitious domain method for particulate flows with heat transfer, J. Comput. Phys., 217 (2005), 424–452.

[29] T. Iwashita, Y. Nakayama and R. Yamamoto, A numerical model for Brownian particles fluctuating in incompressible fluids, J. Phys. Soc. Jpn., 7 (2008), 074007.

[30] R. Benzi, S. Succi and M. R. Vergassola, The lattice Boltzmann equation: theory and applications, Phys. Rep., 222 (1992), 145–197.

[31] S. Y. Chen and G. D. Doolen, Lattice Boltzmann method for fluid flows, Annu. Rev. Fluid. Mech., 30 (1998), 329–364.

[32] M. Wang and N. Pan, Predictions of effective physical properties of complex multiphase materials, Mater. Sci. Eng. Rep., 63 (2008), 1–30.

[33] D. Qi, Lattice-Boltzmann simulations of particles in non-zero-Reynolds-number flows, J. Fluid. Mech., 385 (1999), 41–62.

[34] A. J. C. Ladd and R. Verberg, Lattice-Boltzmann simulations of particle-fluid suspensions, J. Stat. Phys., 104 (2001), 1191–1251.

[35] C. K. Aidun and E.-J. Ding, Dynamics of particle sedimentation in a vertical channel: perioddoubling bifurcation and chaotic state, Phys. Fluids., 15 (2003), 1612–1621.

[36] J. Z. Lin, X. Shi and Z. J. You, Effects of the aspect ratio on the sedimentation of a fiber in Newtonian fluids, J. Aerosol. Sci., 34 (2003), 909–921.

[37] J. Z. Lin, Y. L. Wang and A. O. James, Sedimentation of rigid cylindrical particles with mechanical contacts, Chin. Phys. Lett., 22 (2005), 628–631.

[38] X. Shi, J. Z. Lin and Z. S. Yu, Discontinuous Galerkin spectral element lattice Boltzmann method on triangular element, Int. J. Numer. Methods. Fluids, 42 (2003), 1249–1261.

[39] X. K. Ku and J. Z. Lin, Effect of two bounding walls on the rotational motion of a fiber in the simple shear flow, Fiber. Polym., 10 (2009), 302–309.

[40] Z. H. Xia, K. W. Connington, S. Rapaka, P. T. Yue, J. J. Feng and S. Y. Chen, Flow patterns in the sedimentation of an elliptical particle, J. Fluid. Mech., 625 (2009), 249–272.

[41] Z. G. Feng and E. E. Michaelides, The immersed boundary-lattice Boltzmann method for solving fluid-particles interaction problems, J. Comput. Phys., 195 (2004), 602–628.

[42] Z. G. Feng and E. E. Michaelides, Proteus: a direct forcing method in the simulations of particulate flows, J. Comput. Phys., 202 (2005), 20–51.

[43] X. Shi and N. Phan-Thien, Distributed Lagrange multiplier/fictitious domain method in the framework of lattice Boltzmann method for fluid-structure interactions, J. Comput. Phys., 206 (2005), 81–94.

[44] X. Shi and S. P. Lim, A LBM-DLM/FD method for 3D fluid-structure interactions, J. Comput. Phys., 226 (2007), 2028–2043.

[45] D. M. Nie and J. Z. Lin, A LB-DF/FD method for particle suspensions, Commun. Comput. Phys., 7 (2010), 544–563.

[46] A. Widom, Velocity fluctuations of a hard-core Brownian particle, Phys. Rev. A., 3 (1971), 1394–1396.

[47] E. H. Hauge and A. Martin-Löf, Fluctuating hydrodynamics and Brownian motion, J. Stat. Phys., 7 (1973), 259–281.

[48] E. J. Hinch, Application of the Langevin equation to fluid suspensions, J. Fluid. Mech., 72 (1975), 499–511.

[49] Z. S. Yu and X. M. Shao, A direct-forcing fictitious domain method for particulate flows, J. Comput. Phys., 227 (2007), 292–314.

[50] M. Uhlmann, An immersed boundary method with direct forcing for the simulation of particulate flows, J. Comput. Phys., 209 (2005), 448–476.

[51] H. J. H. Clercx and P. P. J. M Schram, Brownian particles in shear flow and harmonic potentials: a study of long-time tails, Phys. Rev. A., 46 (1992), 1942–1950.